A More Reactive Trigonal-Bipyramidal High-Spin Oxoiron(IV) Complex with a cis-Labile Site

ARTICLE *in* JOURNAL OF THE AMERICAN CHEMICAL SOCIETY · AUGUST 2011

Impact Factor: 12.11 · DOI: 10.1021/ja2040909 · Source: PubMed

8 AUTHORS, INCLUDING:

Yisong Guo
Carnegie Mellon University
31 PUBLICATIONS **483** CITATIONS
SEE PROFILE

Katherine M Van Heuvelen
Harvey Mudd College
17 PUBLICATIONS **306** CITATIONS
SEE PROFILE

Gregory T Rohde
University of Minnesota Twin Cities
11 PUBLICATIONS **301** CITATIONS
SEE PROFILE

Lawrence Que
University of Minnesota Twin Cities
451 PUBLICATIONS **25,695** CITATIONS
SEE PROFILE

Published in final edited form as:
J Am Chem Soc. 2011 August 10; 133(31): 11880–11883. doi:10.1021/ja2040909.

A More Reactive Trigonal Bipyramidal High-Spin Oxoiron(IV) Complex with a *cis*-Labile Site

Jason England[†], **Yisong Guo**[‡], **Katherine M. Van Heuvelen**[†], **Matthew A. Cranswick**[†], **Gregory T. Rohde**[†], **Emile L. Bominaar**[‡,*], **Eckard Münck**[‡,*], and **Lawrence Que Jr.**[†,*]

[†]Department of Chemistry and Center for Metals in Biocatalysis, University of Minnesota, Minneapolis, MN 55455

[‡]Department of Chemistry, Carnegie Mellon University, Pittsburgh, PA 15213

Abstract

The trigonal bipyramidal high-spin (S = 2) oxoiron(IV) complex $[Fe^{IV}(O)(TMG_2dien)(CH_3CN)]^{2+}$ (**7**) was synthesized and spectroscopically characterized. Substitution of the CH_3CN ligand by anions, demonstrated here for X = N_3^- and Cl^-, yielded further S = 2 oxoiron(IV) complexes of general formulation $[Fe^{IV}(O)(TMG_2dien)(X)]^+$ (**7-X**). The reduced steric bulk of **7** relative to the published S = 2 complex $[Fe^{IV}(O)(TMG_3tren)]^{2+}$ (**2**) was reflected by enhanced rates of intermolecular substrate oxidation.

Non-heme monoiron oxygen activating enzymes perform a remarkably diverse array of highly selective oxidative transformations, [1] Most have iron centers with a 2-His-1-carboxylate facial triad structural motif, and their catalytic cycles often involve oxoiron(IV) intermediates as oxidants. Within the past several years, such oxoiron(IV) species have been trapped and spectroscopically characterized in several enzymes and found in all cases to be high spin (S = 2).[2] In contrast, the overwhelming majority of existing synthetic oxoiron(IV) complexes have S = 1 ground states.[3] To date the only published examples of S = 2 oxoiron(IV) complexes are $[Fe^{IV}(O)(H_2O)_5]^{2+}$ (**1**),[4] $[Fe^{IV}(O)(TMG_3tren)]^{2+}$ (**2**, TMG_3tren = 1,1,1-tris{2-[N^2-(1,1,3,3-tetramethylguanidino)]-ethyl}amine))[5] and $[Fe^{IV}(O)(H_3buea)]^-$ (**3**, H_3buea = tris[(*N'-tert*-butylureaylato)-*N*-ethylene]amine trianion).[6] The crystallographically characterized trigonal bipyramidal (TBP) complex **2** was found to react rapidly via intramolecular ligand hydroxylation ($t_{1/2}$ at 25 °C = 30sec), but reacted with external hydrocarbon substrates at rates comparable to those of existing S = 1 complexes. Given that many DFT studies predict more facile H-atom abstraction by S = 2 oxoiron(IV) centers than their S = 1 counterparts,[7] the intermolecular reactivity observed for **2** was disappointingly sluggish, a fact attributed to a steric retardation of reaction due to the bulk of the tetramethylguanidine donors.[5a,8]

In an effort to assess and rationalize the inherent reactivity of the S = 2 oxoiron(IV) center in **2**, we sought to (i) reduce the steric bulk of the supporting ligand and (ii) expand the palette of existing high-spin oxoiron(IV) complexes. Both aims are easily accommodated by replacement of one arm of the tripodal TMG_3tren ligand with a methyl group to yield the tridentate TMG_2dien ligand (Figure 1A).

CORRESPONDING AUTHOR FOOTNOTE eb7g@andrew.cmu.edu; emunck@cmu.edu; larryque@umn.edu.

SUPPORTING INFORMATION PARAGRAPH: Experimental and synthetic details, resonance Raman spectra and additional Xray crystallographic, Mössbauer, EPR, XAS, DFT and kinetics information. This material is available free of charge via the Internet at http://pubs.acs.org.

The iron(II) starting material used in this study, [Fe^{II}(TMG_2dien)($OTf)_2$] (**4**), was prepared by thallium(I) salt metathesis of the chloride ligands in [Fe^{II}(TMG_2dien)($Cl)_2$] (**5**), which was itself generated by combination of equimolar quantities of TMG_2dien and $FeCl_2$. The high-resolution X-ray structures of **4** and **5** (Figures 1B and S1, Tables S1 and S2) reveal 5-coordinate complexes with a geometry that is intermediate between square pyramidal (SP) and TBP (τ = 0.64 and 0.56, respectively). [9] This contrasts with the strictly TBP geometry of [Fe^{II}(TMG_3tren)(OTf)](OTf) (**6**, τ = 0.96), the iron(II) starting material used in the generation of **2**.[5a]

Treatment of a CH_3CN solution of **4** with 2-(*tert*-butylsulfonyl) iodosylbenzene (2-(^{t}BuSO$_2$)C_6H_4IO)[10] yields an orange-brown species **7** ($t_{1/2}$ at −30 °C ≈ 0.5 h *vs*. 4.5 h for **2**) whose electronic spectrum is reminiscent of **2** (Figure 2, Table 1), with a weak near IR (NIR) band centered at 805 nm (270 M^{-1} cm^{-1}) and an intense UV absorption having a shoulder at *ca*. 380 nm (8200 M^{-1} cm^{-1}). Notably, maximization of the intensity of the aforementioned NIR band requires addition of 2.5 – 3 equiv of oxidant. Mössbauer spectroscopy revealed that reaction with a single equivalent of oxidant leads to substoichiometric yields of **7** (45 %), with the remainder of the iron content being associated primarily with unreacted **4** (Figure S2). The absence of other iron products is consistent with non-productive reaction of 2-(^{t}BuSO$_2$)C_6H_4IO due to metal-catalyzed disproportionation, a process that has been documented for this oxidant.[10] Additionally, the ^{19}F NMR spectrum of **7** in CD_3CN displayed a *single* peak at −80 ppm, which is indicative of free triflate and suggests that the potentially *cis*-labile site is filled by a solvent ligand. This observation, combined with the other data detailed herein, leads to formulation of **7** as [Fe^{IV}(O)(TMG_2dien)(CH_3CN)]$^{2+}$.

One of the primary motivations for the development of the chemistry of the TMG_2dien ligand was to generate a TBP high-spin oxoiron(IV) complex incorporating a labile site. To test the viability of our approach, tetraalkylammonium azide and chloride salts were added to pre-formed solutions of iron(IV) complex **7**. This led to near instantaneous UV-Vis spectral changes (Figure 2, Table 1), consistent with substitution of the CH_3CN ligand and formation of new complexes formulated as [Fe^{IV}(O)(TMG_2dien)(X)]$^+$ (**7-X**, X = N_3, Cl), with the resultant spectra retaining the same general features as the parent complex **7** (i.e. a weak NIR band and an intense UV feature that trails into the visible region). Notably, **7-N_3** is of comparable stability to **7**, but **7-Cl** undergoes self-decay at a significantly accelerated rate ($t_{1/2}$ at −30 °C ≈ 34 and 2 min. for **7-N_3** and **7-Cl**, respectively).

The presence of a terminal Fe=O unit in complexes **7**, **7-N_3**, and **7-Cl** was confirmed by resonance Raman spectroscopy (Figure S3), which yielded ν(Fe=O) vibrational modes at 807, 833 and 810 cm^{-1}, respectively. In close agreement with our expectations based upon Hooke's Law ($\Delta\nu$ theoretical ≈ 36 – 37 cm^{-1}), these bands shifted upon ^{18}O-labelling to 773, 795 and 775 cm^{-1}, respectively.

Mössbauer spectroscopy confirms that complexes **7**, **7-N_3**, and **7-Cl** all contain S = 2 oxoiron(IV) centers (Figures 3 (left panel) and S4–S7), with zero-field spectra each exhibiting a doublet with isomer shift δ ≈ 0.1 mm s^{-1} (Table 1). Their distinct quadrupole splittings, ΔE_Q, confirm formation of new anion complexes. The three species were obtained in high yield, with **7**, **7-N_3**, and **7-Cl** accounting for 88, 80 and 87 % (all ca. ±4%) of the Fe present, respectively. Minor iron(III) impurities account for the remainder. Fitting Mössbauer spectra observed at variable applied fields, B, to an S = 2 spin Hamiltonian (see SI) yielded zero-field splitting (ZFS) parameters (D, E/D) and hyperfine parameters that compare well with other S = 2 oxo-iron(IV) species.

The high-spin ground state of **7**, **7-N_3**, and **7-Cl** and the *D* and *E/D* values obtained by Mössbauer spectroscopy were confirmed by parallel mode EPR (Figure 3 (right panel) and S8–S10). The X-band spectra of **7**, **7-N_3** and **7-Cl** all displayed broad resonances at $g \sim 8 - 13$ that originate from the excited state $M_S = \pm 2$ quasi-doublet of an $S = 2$ multiplet. As the intensity of such signals is proportional to $(E/D)^4$, quantitative simulations allowed quite accurate determinations of *E/D* (Table 1).[11]

Consistent with their assignment as oxoiron(IV) complexes, **7**, **7-N_3** and **7-Cl** exhibit XAS edge energies (E_0) of ~7124 eV (Fig. 4, Table 1) that are in the range observed for other oxoiron(IV) complexes and blue-shifted by ≥ 1.7 eV relative to the iron(II) starting material **4** (E_0 = 7121.9 eV). Unlike $S = 1$ oxoiron(IV) complexes, which exhibit a single symmetrical pre-edge feature,[12] **7**, **7-N_3** and **7-Cl** all exhibit pre-edge features composed of two discernible peaks (Figure 4 top and Table S3), originating from 1s→3d electronic transitions. Consequently, two Gaussians are required to model them successfully, as predicted by DFT for high-spin iron(IV) complexes.[13]

Analysis of the EXAFS data for both **7** and **7-Cl** furnished best fits (Tables S4 and S5, Figures 4 and S11) with an O/N scatterer at ~1.65 Å that corresponds to the Fe=O unit. (Thus far, we have been unable to collect high-quality EXAFS data for **7-N_3** due to rapid photo-decomposition.) These distances are comparable to the Fe=O lengths observed in the X-ray structures of **2** and **3** (1.661(2) and 1.680(1) Å, respectively),[5a,6] the EXAFS of enzymatic oxoiron(IV) intermediates,[2e,14b,15] and the plethora of existing $S = 1$ oxoiron(IV) complexes.[3,16] Both **7** and **7-Cl** also have a shell of O/N scatterers at ca. 1.94 Å, four in the former case and three in the latter, assigned to the N-donors of the supporting ligands. This Fe-N distance is shorter than that found for **2** by EXAFS (1.99 Å),[5a] reflecting the lower steric constraints of the TMG_2dien ligand. Lastly, **7-Cl** has a Cl scatterer at 2.27 Å, a distance that is very similar to the 2.31 Å Fe–Cl distance obtained by EXAFS for the chloroferryl intermediate of the α-ketoglutarate-dependent aliphatic halogenase SyrB2.[2e]

DFT calculations for **7**, **7-N_3** and **7-Cl** further support our $S = 2$ spin state assignment for these three complexes (Tables S6– S13). Complex **7**, **7-N_3**, and **7-Cl** all have a ^{5}A ground state with four d electrons located in two half-filled E levels (Table S7). Spin populations calculated for the iron and the oxo atoms, respectively, are +3.0(1) and +0.6(1) (Tables S9 and S10), similar to the values obtained for **1**, **2**, and TauD-J.[4a,5a,14c] The DFT geometry-optimized structures of **7**, **7-N_3** and **7-Cl** (Figures 1C and S12, Table S8) exhibit geometries that are best described as TBP (τ = 0.79, 0.83 and 0.72, respectively)[9] and have Fe=O bond lengths of ~1.65 Å, in close agreement with values obtained from EXAFS. In contrast, the Fe-Cl distance of 2.35 Å calculated for **7-Cl** is somewhat longer than the value of 2.27 Å determined by EXAFS. Lastly, the DFT-calculated spin-dipolar contribution to the ^{57}Fe *A*-tensor is in good agreement with the experimental data (Table S6), indicating that the z axis of the spin Hamiltonian (determined by the ZFS tensor) is oriented along the Fe-O bond (within about 5°).

In addition to creating a $S = 2$ oxoiron(IV) complex with a *cis*-labile site, it was anticipated that removing one of the bulky tetramethylguanidinyl donors of the TMG_3tren ligand to give TMG_2dien would provide substrates greater access to the Fe^{IV}=O unit, thereby allowing the inherent reactivity properties of the $S = 2$ oxoiron(IV) center to be manifested. Consistent with these expectations, the oxo-transfer reaction of **7** to PPh_3 proceeded so rapidly that we were unable to accurately measure the associated rate constants at −30 °C for comparison with published data for other oxoiron(IV) complexes listed in Table 2. Additionally, H-atom abstraction from 1,4-cyclohexadiene (CHD) and 9,10-dihydroanthracene (DHA), substrates with similarly weak C–H bonds but differing steric profiles, proceeded at comparable rates,

with respective second-order rate constants 15 and 630 times larger than for the more sterically hindered **2** (Table 2, Figures S13–S15).

Notably, **7** exhibits reactivity more than one and three orders of magnitude greater than the *S* = 1 complexes $[Fe^{IV}(O)(N4Py)]^{2+}$ (**8**) and $[Fe^{IV}(O)(TMC)(CH_3CN)]^{2+}$ (**9**) (Table 2), respectively, which would appear to support DFT-based predictions of a more reactive *S* = 2 Fe^{IV}=O center relative to a *S* = 1 Fe^{IV}=O center.[7] However, **7** is an order of magnitude less reactive than the recently reported *S* = 1 complex $[Fe^{IV}(O)(Me_3NTB)]^{2+}$ (**10**).[17] This fact serves to highlight the difficulty of making such comparisons without consideration of the thermodynamic and steric consequences of the differing ligand environments of the various complexes. Thus far, there is only one pair of closely related complexes that have identical ligand environments, namely $[(HO)(L)Fe^{III/IV}–O–Fe^{IV}(L)(O)]$ where L = tris(3,5-dimethyl-4-methoxypyridyl–2-methyl)amine, but differ in having a *S* = 1 or *S* = 2 oxoiron(IV) unit.[18] Remarkably, the high-spin $Fe^{III}Fe^{IV}$ complex was found to be a thousandfold more reactive than the low-spin $Fe^{IV}Fe^{IV}$ complex, thereby providing support for the DFT-based predictions.

In summary, we have described the synthesis of the high-spin oxoiron(IV) complex $[Fe^{IV}(O)(TMG_2dien)(CH_3CN)]^{2+}$ (**7**), which is related to the *S* = 2 complex $[Fe^{IV}(O)(TMG_3dien)(CH_3CN)]^{2+}$ (**2**) by replacement of one of the tetramethylguanidinyl arms of the TMG_3tren ligands by a methyl group and inclusion of a solvent ligand in its place. This modification provides greater access to the Fe^{IV}=O subunit, eliminating the selectivity for smaller substrates exhibited by **2** and resulting in a significant increase in the rates of intermolecular reactions. Furthermore, the introduction of CH_3CN as an equatorial ligand in **7** provides a means to access a series of closely related anion substituted *S* = 2 oxoiron(IV) complexes that are highly amenable to characterization, as illustrated here for $[Fe^{IV}(O)(TMG_2dien)(X)]^{+}$ (**7-X**, X = N_3, Cl). This offers the promise of elucidating spectroscopic and reactivity trends as a function of the electronic properties of an *S* = 2 oxoiron(IV) center and may provide answers to specific bio-relevant questions, such as the reason for the omnipresence of carboxylato ligands in non-heme enzymes[1] and for the inherent preference for halogen versus oxygen atom rebound in non-heme iron halogenase enzymes. [19]

Supplementary Material

Refer to Web version on PubMed Central for supplementary material.

Acknowledgments

This work was supported by the NIH (grants GM33162 to LQ and EB001475 to EM and postdoctoral fellowships ES017390 to MAC and GM093479 to KMVH) and the NSF (grants CHE1058248 to LQ and CHE070073 to ELB through Teragrid resources provided by NCSA). XAS data were collected on beamline X3B at the National Synchrotron Light Source (NSLS), Brookhaven National Laboratory. NSLS is supported by the U.S. Department of Energy, Office of Science, Office of Basic Energy Sciences, under Contract No. DE-AC02-98CH10886. We thank Michael Sullivan for technical assistance with our XAS experiments. Data collection and structure solution were conducted by Victor G. Young, Jr. at the X-Ray Crystallographic Laboratory, Department of Chemistry, University of Minnesota.

REFERENCES

1. (a) Krebs C, Galonić Fujimori D, Walsh CT, Bollinger JM Jr. Acc. Chem. Res. 2007; 40:484–492. [PubMed: 17542550] (b) Kovaleva EG, Lipscomb JD. Nat. Chem. Biol. 2008; 4:186–193. [PubMed: 18277980]
2. (a) Eser BE, Barr EW, Frantom PA, Saleh L, Bollinger JM Jr, Krebs C, Fitzpatrick PF. J. Am. Chem. Soc. 2007; 129:11334–11335. [PubMed: 17715926] (b) Price JC, Barr EW, Tirupati B, Bollinger JM Jr, Krebs C. Biochemistry. 2003; 42:7497–7508. [PubMed: 12809506] (c) Hoffart

LM, Barr EW, Guyer RB, Bollinger JM Jr, Krebs C. Proc. Natl. Acad. Sci. U.S.A. 2006; 103:14738–14743. [PubMed: 17003127] (d) Galonić DP, Barr EW, Walsh CT, Bollinger JM Jr, Krebs C. Nat. Chem. Biol. 2007; 3:113–116. [PubMed: 17220900] (e) Matthews ML, Krest CM, Krest CM, Barr EW, Vaillancourt FH, Walsh CT, Green MT, Krebs C, Bollinger JM Jr. Biochemistry. 2009; 48:4331–4343. [PubMed: 19245217]

3. Que L Jr. Acc. Chem. Res. 2007; 40:493–500. [PubMed: 17595051]
4. Pestovsky O, Stoian S, Bominaar EL, Shan X, Münck E, Que L Jr, Bakac A. Angew. Chem., Int. Ed. 2005; 44:6871–6874.
5. (a) England J, Martinho M, Farquhar ER, Frisch JR, Bominaar EL, Münck E, Que L Jr. Angew. Chem., Int. Ed. 2009; 48:3622–3626.(b) England J, Guo Y, Farquhar ER, Young VG Jr, Münck E, Que L Jr. J. Am. Chem. Soc. 2010; 132:8635–8644. [PubMed: 20568768]
6. Lacy DC, Gupta R, Stone KL, Greaves J, Ziller JW, Hendrich MP, Borovik AS. J. Am. Chem. Soc. 2010; 132:12188–12190. [PubMed: 20704272]
7. (a) Ye S, Neese F. Curr. Opin. Chem. Biol. 2009; 13:89–98. [PubMed: 19272830] (b) Decker A, Rohde J-U, Klinker EJ, Wong SD, Que L Jr, Solomon EI. J. Am. Chem. Soc. 2007; 129:15983–15996. [PubMed: 18052249] (c) Bernasconi L, Louwerse MJ, Baerends EJ. Eur. J. Inorg. Chem. 2007:3023–3033.(d) Hirao H, Kumar D, Que L Jr, Shaik S. J. Am. Chem. Soc. 2006; 128:8590–8606. [PubMed: 16802826]
8. (a) Janardanan D, Wang Y, Schyman P, Que L Jr, Shaik S. Angew. Chem., Int. Ed. 2010; 49:3342–3345.(b) Wong SD, Bell CB III, Liu LV, Kwak Y, England J, Zhao J, Que L Jr, Solomon EI. Angew. Chem. Int. Ed. 2011; 50:3215–3218.
9. Addison AW, Rao TN, Reedijk J, Van Rijn J, Verschoor GC. J. Chem. Soc., Dalton Trans. 1984:1349–1356.
10. Macikenas D, Skrzypczak-Jankun E, Protasiewicz JD. J. Am. Chem. Soc. 1999; 121:7164–7165.
11. Surerus KK, Hendrich MP, Christie PD, Rottgardt D, Orme-Johnson WH, Münck E. J. Am. Chem. Soc. 1992; 114:8579–8590.
12. (a) Jackson TA, Rohde JU, Seo MS, Sastri CV, DeHont R, Stubna A, Ohta T, Kitagawa T, MAünck E, Nam W, Que L Jr. J. Am. Chem. Soc. 2008; 130:12394–12407. [PubMed: 18712873] (b) Rohde J-U, Torelli S, Shan X, Lim MH, Klinker EJ, Kaizer J, Chen K, Nam W, Que L Jr. J. Am. Chem. Soc. 2004; 126:16750–16761. [PubMed: 15612713]
13. Berry JF, DeBeer George S, Neese F. Phys. Chem. Chem. Phys. 2008; 10:4361–4374. [PubMed: 18654674]
14. (a) Proshlyakov DA, Henshaw TF, Monterosso GR, Ryle MJ, Hausinger RP. J. Am. Chem. Soc. 2004; 126:1022–1023. [PubMed: 14746461] (b) Riggs-Gelasco PJ, Price JC, Guyer RB, Brehm JH, Barr EW, Bollinger JM Jr, Krebs C. J. Am. Chem. Soc. 2004; 126:8108–8109. [PubMed: 15225039] (c) Sinnecker S, Svensen N, Barr EW, Ye S, Bollinger JM Jr, Neese F, Krebs C. J. Am. Chem. Soc. 2007; 129:6168–6179. [PubMed: 17451240]
15. Fujimori DG, Barr EW, Matthews ML, Koch GM, Yonce JR, Walsh CT, Bollinger JM Jr, Krebs C, Riggs-Gelasco PJ. J. Am. Chem. Soc. 2007; 129:13408–13409. [PubMed: 17939667]
16. (a) Rohde J-U, In J-H, Lim MH, Brennessel WW, Bukowski MR, Stubna A, Münck E, Nam W, Que L Jr. Science. 2003; 299:1037–1039. [PubMed: 12586936] (b) Klinker EJ, Kaizer J, Brennessel WW, Woodrum NL, Cramer CJ, Que L Jr. Angew. Chem., Int. Ed. 2005; 44:3690–3694.(c) Thibon A, England J, Martinho M, Young VG Jr, Frisch JR, Guillot R, Girerd J-J, Münck E, Que L Jr, Banse F. Angew. Chem., Int. Ed. 2008; 47:7064–7067.
17. Seo MS, Kim NH, Cho K-B, So JE, Park SK, ClAémancey M, Garcia-Serres R, Latour J-M, Shaik S, Nam W. Chem. Sci. 2011; 2:1039–1045.
18. Xue G, De Hont R, Münck E, Que L Jr. Nat. Chem. 2010; 2:400–405. [PubMed: 20414242]
19. (a) Matthews ML, Neumann CS, Miles LA, Grove TL, Booker SJ, Krebs C, Walsh CT, Bollinger JM Jr. Proc. Natl. Acad. Sci. U.S.A. 2009; 106:17723–17728. [PubMed: 19815524] (b) de Visser SP, Latifi R. J. Phys. Chem. B. 2008; 113:12–14. [PubMed: 19061416] (c) Kulik HJ, Blasiak LC, Marzari N, Drennan CL. J. Am. Chem. Soc. 2009; 131:14426–14433. [PubMed: 19807187] (d) Borowski T, Noack H, RadonÌ M, Zych K, Siegbahn PEM. J. Am. Chem. Soc. 2010; 132:12887–12898. [PubMed: 20738087] (e) Pandian S, Vincent MA, Hillier IH, Burton NA. Dalton Trans. 2009:6201–6207. [PubMed: 20449117]

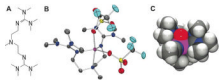

Figure 1.

A: Structure of TMG_2dien ligand. **B**: Thermal ellipsoid plot of [Fe^{II}(TMG_2dien)($OTf)_2$] (**4**), showing 50% probability ellipsoids. Hydrogen atoms have been omitted for clarity. Selected bond distances (Å): Fe-O_{axial}, 2.2012(15); Fe-$O_{equatorial}$, 2.0816(15); Fe-N_{axial}, 2.2835(17); Fe-$N_{guanidine}$(ave), 2.0597(17). **C**: Space-filling model of DFT-generated structure of **7**. Atom color scheme: C, gray; F, light blue; Fe, magenta; H, white; N, blue; O, red; S, yellow.

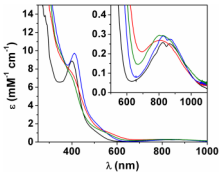

Figure 2.
Main: electronic spectra of **2** (black line), **7** (red line), **7-N_3** (blue line) and **7-Cl** (green line) in CH_3CN solution. Inset: expansion of the NIR region features.

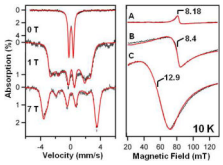

Figure 3.

Left panel: Selected 4.2 K Mössbauer spectra of **7** in CH_3CN (black) recorded in parallel applied magnetic fields, as indicated. For all spectra, a high-spin Fe^{III} impurity, representing ~ 12% of the iron, has been subtracted from the raw data. Solid red lines are spectral simulations using the parameters in Table 1. Additional spectra are shown in Figures S4 – S7. Right panel: X-band EPR spectra (black) of (**A**) **7-N$_3$**, (**B**) **7**, and (**C**) **7-Cl**. Red lines are spectral simulations for (**A**) $D = 5.0\ cm^{-1}$, $E/D = 0.05$, $\sigma_{E/D} = 0.02$; (**B**) $D = 4.2\ cm^{-1}$, $E/D = 0.1$, $\sigma_{E/D} = 0.03$; (**C**) $D = 4.2\ cm^{-1}$, $E/D = 0.14$, $\sigma_{E/D} = 0.016$. In all simulations, intrinsic g values were kept isotopic ($g_x = g_y = g_z = 2$). $\sigma_{E/D}$ is the width of an assumed Gaussian distribution of E/D. Additional spectra are shown in Figures S8 – S10. Experimental conditions: $B_1 \| B$; temperature, 10 K; microwave power, 2 mW (for **B** and **C**) and 20 mW (for **A**) at 9.28 GHz.

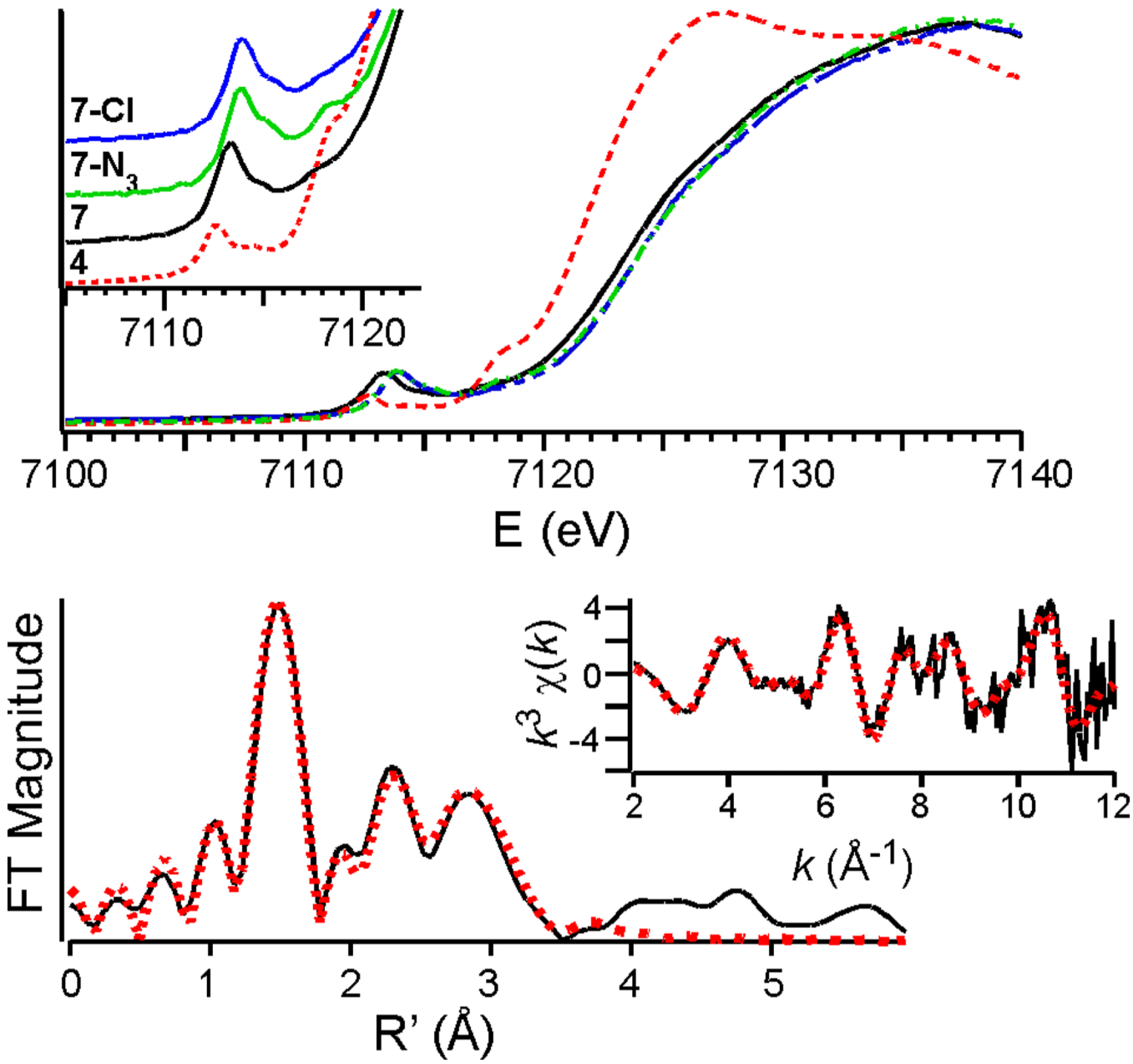

Figure 4.

Top: X-ray absorption edge spectra of **4** (red), **7** (black), **7-N$_3$** (green), and **7-Cl** (blue). Inset: Expansion of the pre-edge region. Bottom: Fe *K*-edge unfiltered EXAFS data ($k^3\chi$ (*k*), inset) and the corresponding Fourier transform for **7-Cl**. The red dots and solid black lines correspond to the experimental data and fits, respectively. Fit of **7** and further details of the EXAFS analysis are provided in the Supporting Information.

Table 1

Spectroscopic parameters of selected *S* = 2 oxoiron(IV) complexes.

Complex	λ_{max} [nm] (ε_{max} [M cm^{-1}])	νFe=O [cm^{-1}]	*D* [cm^{-1}]	*E*/*D*	$A_{x,y,z}/g_n\beta_n$ [T]	ΔE_Q [mm s^{-1}]	η	δ [mm s^{-1}]	E_0 [eV]	E_{PE} [eV] (area)
7	380 (8200),[a] 805 (270)	808	4.5[b] 4.2[c]	0.09[b] 0.10[c]	−13.9, −15.8, −26.0	0.58[d]	0.5	0.08	7123.6	7113.3 (19.9), 7115.0 (3.1)
7-N$_3$	412 (9700), 827 (290), 867 (275)	833	4.6[b] 5.0[c]	0.04[b] 0.05[c]	−15.5, −14.5, −27.0	−0.30[e]	0.35	0.12	7124.2	7113.8 (24.7), 7115.7 (9.2),
7-Cl	385 (7800),[a] 803 (295), 825 (293)	810	4.1[b] 4.2[c]	0.13[b] 0.14[c]	−15.1, −15.4, −26.6	0.41	0.53	0.08	7123.9	7113.9 (21.9), 7115.7 (2.1)
2[f]	400 (8900), 825 (260), 865 (250)	843	5.0	0.02	−15.5, −14.8, −28.0	−0.29	0	0.09	7123.2	7113.8 (23.9), 7115.6 (3.1)
3[g]	350 (4200), 440 (3100), 550 (1900), 808 (280)	798	4.0	0.03	-	0.43	-	0.02	-	-
1[h]	320	-	9.7	0	−20.3, −20.3, nd	−0.33	0	0.38	7126	60–70
TauD-J[i]	318	821	10.5	0.01	−18.4, −17.6, −31.0	−0.9	0	0.30	7123.8[j]	

[a] Shoulder.

[b] Determined by Mössbauer spectroscopy.

[c] Determined by EPR.

[d] The electric field gradient (EFG) tensor and the *A*-tensor are rotated relative to the ZFS tensor by α_{EFG} = 50°, β_{EFG} = 45° and α_A = 55° (WMOSS convention); see SI for comments.

[e] The EFG tensor and the *A*-tensor are rotated by α_{EFG} = 30°, β_{EFG} = 60° and α_A = 20°.

[f] Reference 5a.

[g] Reference 6.

[h] Reference 4.

[i] Data from references 2b and 14.

[j] Assuming an Fe foil reference *E* of 7112.0 eV.

J Am Chem Soc. Author manuscript; available in PMC 2012 August 10.

Table 2

Second-order rate constants (k_2) observed in reactions of Fe^{IV}=O complexes with substrates.

Complex [a]	k_2 [M^{-1} s^{-1}] in CH_3CN solution at −30°C [b]		
	CHD	DHA	PPh_3
7	18	57	*c*
2 [d]	1.2	0.090	1.1
8 [d]	1.3	2.0	1.5
9 [d]	0.018	0.016	0.22
10 [e]	94	310	*c*

[a] $[Fe^{IV}(O)(N4Py)]^{2+}$ (**8**, N4Py = bis(2-pyridylmethyl)-bis(2-pyridyl)-methylamine), $[Fe^{IV}(O)(TMC)(CH_3CN)]^{2+}$ (**9**, TMC = 1,4,8,11-tetramethylcyclam), $[Fe^{IV}(O)(Me_3NTB)]^{2+}$ (**10**, Me_3NTB = tris((N-methyl-benzimidazol-2-yl)methyl)amine)).

[b] Reaction kinetics for **2**, **8** and **9** were measured using 1.0 mM complex. For **7** the larger rates of reaction required the use of 0.1–0.2 mM complex and similarly reduced concentrations of substrate.

[c] This reaction was too fast for measurement of k_{obs}.

[d] Kinetic data from reference 5a.

[e] Kinetic data at −40 °C taken from reference 17.